Size-dependent surface tension of a cylindrical nanobubble in liquid Ar

2012 Chinese Phys. B 21 083102

(http://iopscience.iop.org/1674-1056/21/8/083102)

Size-dependent surface tension of a cylindrical nanobubble in liquid Ar*

Yan Hong(闫 红)[a)b)], Zhu Ru-Zeng(朱如曾)[a)†], and Wei Jiu-An(魏久安)[a)c)]

[a)] *State Key Laboratory of Nonlinear Mechanics (LNM), Institute of Mechanics, Chinese Academy of Sciences, Beijing* 100190, *China*

[b)] *Department of Electronic Information and Physics, Changzhi University, Changzhi* 046011, *China*

[c)] *Advanced Semiconductor Materials (ASM) Technology Singapore,* 2 *Yishun Avenue* 7, *Singapore* 768924

(Received 27 December 2011; revised manuscript received 13 February 2012)

In view of the continued disputes on the fundamental question of whether the surface tension of a vapour bubble in liquid argon increases, or decreases, or remains unchanged with the increase of curvature radius, a cylindrical vapour bubble of argon is studied by molecular dynamics simulation in this paper instead of spherical vapour bubble so as to reduce the statistical error. So far, the surface tension of the cylindrical vapour bubble has not been studied by molecular dynamics simulation in the literature. Our results show that the surface tension decreases with radius increasing. By fitting the Tolman equation with our data, the Tolman length $\delta = -0.6225$ sigma is given under cut-off radius 2.5σ, where $\sigma = 0.3405$ nm is the diameter of an argon atom. The Tolman length of Ar being negative is affirmed and the Tolman length of Ar being approximately zero given in the literature is negated, and it is pointed out that this error is attributed to the application of the inapplicable empirical equation of state and the neglect of the difference between surface tension and an equimolar surface.

Keywords: cylindrical nanobubble, surface tension, Tolman length, molecular dynamics simulation

PACS: 31.15.xv, 68.03.Cd, 68.35.Md **DOI:** 10.1088/1674-1056/21/8/083102

1. Introduction

The theoretical and practical significance of nanobubble study is remarkable. It has a profound influence on surface science, fluid dynamics, MEMS, bioscience, and some application areas.[1,2] In the phase transition processes occurring in many kinds of heat and mass transfers, many vapour bubbles are formed including macroscopic and nanoscopic ones, and all the macroscopic vapour bubbles must pass through the nanobubble stage in the early stages of the nucleation process. Therefore nanobubble research is of great significance for increasing the basic understanding of transfer processes and their application to engineering. The relations between surface tension and curvature radius have a decisive effect on the action of nanobubbles.[3,4]

Tolman's[5,6] thermodynamic theory indicated that the surface tension $\gamma(R_\mathrm{s})$ of a spherical interface is dependent on the radius of surface of tension R_s. Tolman obtained an equation, subsequently named the Gibbs–Tolman–Koening–Buff equation, as follows:

$$\frac{1}{\gamma_\mathrm{s}}\frac{\mathrm{d}\gamma_\mathrm{s}}{\mathrm{d}R_\mathrm{s}} = \frac{\left(2\delta/R_\mathrm{s}^2\right)\left[1+\delta/R_\mathrm{s}+\left(\delta/R_\mathrm{s}\right)^2/3\right]}{1+\left(2\delta/R_\mathrm{s}\right)\left[1+\delta/R_\mathrm{s}+\left(\delta/R_\mathrm{s}\right)^2/3\right]}, \quad (1)$$

where Tolman length δ is defined as

$$\delta(R_\mathrm{s}) = R_\mathrm{e} - R_\mathrm{s}, \quad (2)$$

with R_e being the radius of the equimolar surface. Equation (1) is not self-consistent, for it has two unknown functions $\gamma(R_\mathrm{s})$ and $\delta(R_\mathrm{s})$, but only one equation exists. Tolman pointed out that if we neglect higher order terms and treat δ as a constant δ_∞ for the big radius in Eq. (1), it has an approximate solution

$$\frac{\gamma_\mathrm{s}}{\gamma_\infty} = \frac{1}{1+2\delta_\infty/R_\mathrm{s}} + \cdots = 1 - \frac{2\delta_\infty}{R_\mathrm{s}} + \cdots, \quad (3)$$

which is called the Tolman equation. Equation (3) shows that whether $\gamma(R_\mathrm{s})$ increases or decreases with R_s increasing under the first approximation depends on whether δ_∞ is positive or negative, and the significant level degree is indicated by δ_∞.

*Project supported by the National Natural Science Foundation of China (Grant No. 11072242).

†Corresponding author. E-mail: zhurz@lnm.imech.ac.cn

The investigated objects on the relation between $\gamma(R_{\rm s})$ and $R_{\rm s}$ at nanosize are mainly liquid drops, next gas bubbles,[7] and the research on vapour bubbles is fewest. This is because the number of molecules in bubbles is so small, especially in vapour bubbles, that the accuracy of experimental and MD studies cannot be satisfied.[8] In the literature about δ_∞, some results are unsatisfied or even wrong. For example, in Ref. [9], the treatment is wrong in both mathematical and physical aspects. We have corrected it.[10] This shows the difficulty of studying δ_∞.

Our attention in the present paper is concentrated on the relation between the surface tension and the radius for nano vapour bubbles in liquid Ar. Park *et al.*'s work[11] in 2001 is the first molecular dynamics (MD) study on the surface tension of bubbles. They found that the surface tension of vapour bubbles of liquid argon decreases with radius increasing and from their data, we can obtain Tolman length δ_∞ to be about -0.75. However, strong disagreement about this still exists. In 2008, in order to overcome the difficulty that the vapour density is so low that the statistics is too poor to calculate pressure directly, Matsumoto and Tanaka[1] used the vapour pressure determined by the vapour density through the empirical equation of state given by their MD simulation for the bulk vapour phase. Their MD study results of vapour bubbles of liquid argon showed that the surface tensions of nano vapour bubbles are nearly the same as that of a planar interface,[1] which means that Tolman length is nearly zero. How to solve this contradiction is an intractable problem.

One of the causes of above difference may lie in the fact that the system size is so tiny that the statistical error is too large. The quantity of vapour in a cylindrical vapour bubble is much bigger than that in a spherical bubble with the same radius so that the statistical error is less for the former than for the latter. Therefore in the present paper we take a cylindrical nano vapour bubble instead of a spherical nano vapour bubble as an object to be investigated. Besides, so far the surface tension of cylindrical nano vapour bubbles has not been reported in the literature.

The rest of the present paper is organized as follows. In Section 2, we propose the theoretical basis and calculation scheme. In Section 3 we describe the simulation, results, and discussion. In Section 4 we give an explanation of the origin of the difference in Tolman length between our results and the data given in the literature. The conclusion is given in Section 5.

2. Theoretical basis and calculation scheme

For cylindrical vapour bubbles, the Tolman equation (3) should be replaced by Tolman equation[12]

$$\frac{\gamma_{\rm s}}{\gamma_\infty} = \frac{1}{1+\delta_\infty/R_{\rm s}}. \tag{4}$$

To fit this equation, we need to calculate the tension of planar interface γ_∞ and those of cylindrical vapour bubbles with different values of radius $\gamma_{\rm s}$ by MD simulations. To this end we must have some equations for cylindrical vapour bubbles and a planar interface.

2.1. Some equations for cylindrical vapour bubbles

Now, we consider a single-component cylindrical vapour bubble. In cylindrical coordinates the pressure tensor is written in the form of

$$\overline{\overline{P}} = p_{\rm N}(r)\,\boldsymbol{e}_r\boldsymbol{e}_r + p_{\rm T}(r)\left[\boldsymbol{e}_\theta\boldsymbol{e}_\theta + \boldsymbol{e}_z\boldsymbol{e}_z\right], \tag{5}$$

where $\boldsymbol{e}_r$, $\boldsymbol{e}_\theta$, and $\boldsymbol{e}_z$ are orthogonal unit vectors, and $p_{\rm N}(r)$ and $p_{\rm T}(r)$ are the normal and transverse component of the pressure tensor, respectively.

In Ref. [13] the expressions of the radius and surface tension for surface tension in terms of pressure distribution are given for cylindrical liquid drops. Exchanging the positions of vapour and liquid in these expressions, we can obtain the expressions for cylindrical vapour bubbles as follows:

$$\gamma_{\rm s}^2 = -\left(p^v - p^l\right)\int_{R^v}^{R^l} r^2\frac{{\rm d}p_{\rm N}(r)}{{\rm d}r}\,{\rm d}r, \tag{6}$$

where R^v and R^l denote the radii of cylindrical surfaces inside a homogeneous vapour phase and inside a homogeneous liquid phase with the z axis being their symmetrical axis, respectively, and p^v and p^l are the pressures $p_{\rm N}(R^v)$ and $p_{\rm N}(R^l)$, respectively. Because of the isotropy of the pressure tensor in the bulk phase, Eq. (6) gives the same result for any pair of R^l and R^v in the bulk phase. Besides, Laplace equation[12]

$$p^v - p^l = \frac{\gamma_{\rm s}}{R_{\rm s}} \tag{7}$$

gives

$$R_{\rm s} = \frac{\gamma_{\rm s}}{p^v - p^l}. \tag{8}$$

To be suitable for MD simulation, Eq. (6) can be transformed into the following form:

$$\gamma_{\rm s}^2 = -(p^v - p^l)\left[(p^v)^2 - (p^l)^2 - 2\int_{R^v}^{R^l} p_{\rm N}(r) r\,{\rm d}r\right]. \tag{9}$$

Having obtained the pressure distribution of $p_{\rm N}(r)$ by MD simulation, we can substitute $p_{\rm N}(r)$ into Eq. (9) to obtain $\gamma_{\rm s}$. Then by substituting $\gamma_{\rm s}$, p^v, and p^l into Eq. (8), the radius of the surface tension $R_{\rm s}$ is given.

2.2. Some equations for planar interface

We know that the tension of a planar interface is independent of the selection of dividing surface. For the planar interface parallel to the xy plane, the tension is determined by[6]

$$\gamma_\infty = \int_{z_l}^{z_v} {\rm d}z \left\{p_{\rm N}(z) - p_{\rm T}(z)\right\}, \tag{10}$$

where $p_{\rm N}(z)$ and $p_{\rm T}(z)$ are the normal and tangential component of the pressure tensor, respectively, and z_l and z_v are coordinates of an arbitrary position in the bulk liquid and in the bulk vapour outside the transition layer, respectively.

If the particle number of a system is insufficient when the planar interface is simulated, interface fluctuation is liable to be caused. A double-interface system as shown in Fig. 1, is generally chosen to reduce errors. Then the expression of surface tension is

$$\gamma_\infty = \frac{1}{2}\int_{z_{v1}}^{z_{v2}} {\rm d}z \left\{p_{\rm N}(z) - p_{\rm T}(z)\right\}, \tag{11}$$

where z_{v1} and z_{v2} are the coordinates in the different vapour phases, respectively.

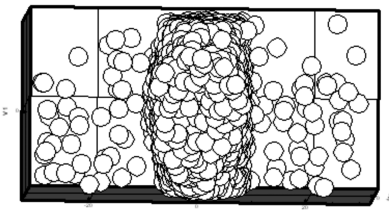

Fig. 1. A double planar vapour–liquid interface system at $T^* = 0.75$.

2.3. Line for realization of general goal

After the values of radius $R_{\rm s}$ and the surface tension $\gamma_{\rm s}$ of several cylindrical vapour bubbles with different sizes and the surface tension γ_∞ of planar interface are calculated according to the foregoing route, we use Tolman Eq. (4) for the cylindrical interface to calculate the Tolman lengths δ_∞ for our simulated systems one by one, and then obtain their average Tolman length $\bar{\delta}_\infty$. Of course, we can also fit the values of four different bubble systems and the planar interface system to Eq. (4) to obtain a more reliable Tolman length $\bar{\delta}_\infty$, however, the difference is slight.

3. MD simulation, results, and discussion

A double-interface system of liquid argon and its vapour at $T = 90$ K is shown in Fig. 1 and several cylindrical nano vapour bubbles formed in liquid argon at $T = 90$ K, as shown in Fig. 2, are simulated. We use canonical ensemble (N, V, T constant) MD simulation.

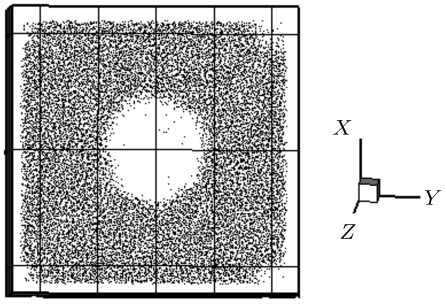

Fig. 2. A cylindrical vapour bubble of particle number $N = 19656$ at $T^* = 0.75$.

The intermolecular interactions between argon atoms are described by the Lennard–Jones potential

$$U(r) = 4\varepsilon\left\{\left(\frac{\sigma}{r}\right)^{12} - \left(\frac{\sigma}{r}\right)^{6}\right\} \tag{12}$$

with cut-off distance $r_{\rm c} = 2.5\sigma$, where r, ε, and σ are the interparticle distance, energy scale, and length scale, respectively. All quantities used in the simulation are dimensionless and are expressed by adding superscript *. According to the basic parameters of an argon atom, $m = 6.63382 \times 10^{-26}$ g, $\varepsilon = 120Kk_{\rm B}$ ($k_{\rm B} = 1.38 \times 10^{-23}$ J/K), $\sigma = 0.3405$ nm, the dimensionless quantities are as follows:

$r^* = r/\sigma$ for length,
$T^* = k_{\rm B}T/\varepsilon$ for temperature,
$t^* = t\sqrt{(\varepsilon/m\sigma^2)}$ for time,
$\rho^* = \rho\sigma^3/m$ for density,
$f^* = f\sigma/\varepsilon$ for force, and $E^* = E/\varepsilon$ for energy.

The simulated temperature is $T^* = 0.75$. For the cylindrical vapour bubble systems and planar interface system, at the initial time all the particles are given velocities according to the Maxwell–Boltzmann distribution. The velocity–Verlet algorithm is used in MD.[14] The canonical ensemble (NVT ensemble) of temperature 90 K and the time step $\delta t = 5$ fs are used before equilibrium.

On calculating the mean value of a physical quantity, we change the time step into $\delta t = 2$ fs. In order to find the step number N that is needed for a physical

quantity, say, $g(t)$ to reach its steady value, we use an accumulative average method[15] for the statistics

$$\overline{g(i\delta t)}^N = \frac{1}{N}\sum_{i=1}^{N} g(i\delta t). \tag{13}$$

The typical behaviour of $\overline{g(i\delta t)}^N$ is shown in Fig. 3, from which the step number N needed for the accumulative average to reach the steady value is easily found to be 4×10^5.

The simulations of the planar interface system and the cylindrical vapour bubble system are described respectively as follows.

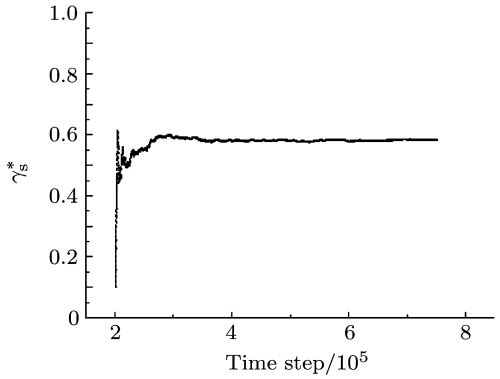

Fig. 3. Relation between the accumulative average of γ_s and the time step for the planar vapour–liquid interface.

3.1. Simulation of the planar vapour–liquid interface system

The box size of simulation system is $x^*\times y^*\times z^* = 30.0\times30.0\times60.0$. Because the vapour density is far smaller than liquid density, the total number of particles of liquid is approximately equal to the sum of particle numbers of liquid and vapour. Therefore the total number of particles can be estimated according to the density of liquid Ar at $T = 90$ K, the box size and the approximate thickness of liquid. In this way, the initial configuration is constructed by putting $24\times24\times22 = 12672$ particles on a finite cubic lattice located at the central part of the box, and so the atomic separation is a bit larger than 1σ. The periodic boundary condition is used in all directions. The double planar vapour–liquid interface system is formed when the system is in equilibrium after relaxation process. A double planar vapour–liquid interface system at $T^* = 0.75$ is shown in Fig. 1.

To calculate the normal and tangential components of the pressure tensor of the double planar vapour–liquid interface system, we divide the simulation domain of $L_x^*\times L_y^*\times L_z^* = 30.0\times30.0\times60.0$ equally into 30 slabs perpendicular to the interface. The thickness of each slab is $\Delta z = 2.0$. Slabs are specified with $k = 1,\ldots$. The statistical expressions of the normal and tangential components of the pressure tensor are[11]

$$p_{\mathrm{N}}^*(k) = \langle n^*(k)\rangle T^* - \frac{1}{L_x^*L_y^*\Delta z} \times\left\langle\sum_{i,j}\frac{z_{ij}^{*2}}{r_{ij}^*}U^{*\prime}\left(r_{ij}^*\right)f_{k,ij}\right\rangle, \tag{14}$$

and

$$p_{\mathrm{T}}^*(k) = \langle n^*(k)\rangle T^* - \frac{1}{L_x^*L_y^*\Delta z^*} \times\left\langle\sum_{i,j}\frac{\left(x_{ij}^{*2}+y_{ij}^{*2}\right)/2}{r_{ij}^*}U^{\prime *}\left(r_{ij}^*\right)f_{k,ij}\right\rangle, \tag{15}$$

where the symbol $\langle\ \rangle$ denotes the time average. On the right-hand side of each of the above two equations, the first term is a kinetic term and the second is a configuration term, $n^*(z)$ is the particle density, $U^*\left(r_{ij}^*\right)$ is the interparticle potential function, x_{ij}^*, y_{ij}^*, and r_{ij}^* are the relative coordinates and distance between particles i and j with effective interaction, respectively, and $f_{k,ij}$ is the length fraction of the link between i and j in slab k. Substituting Eqs. (14) and (15) into Eq. (11), we have

$$\gamma_\infty^* = \frac{1}{2L_x^*L_y^*}\left\langle\sum_{i,j}\frac{\left(x_{ij}^{*2}+y_{ij}^{*2}\right)/2-z_{ij}^{*2}}{r_{ij}^*}U^{*\prime}\left(r_{ij}^*\right)f_{ij}\right\rangle, \tag{16}$$

where f_{ij} is the length fraction of the link between particles i and j in the simulation domain of $L_x^*\times L_y^*\times L_z^* = 30.0\times30.0\times60.0$. Figure 3 shows the change of the accumulative average of the surface tension of the planar vapour–liquid interface with time step according to our simulation for Eq. (16). We see that when the time step is equal to 4×10^5, the accumulative average reaches a stable value. The average surface tension of the planar vapour–liquid interface is $\gamma_\infty^* = 0.5896$. This is close to the results given in Refs. [11] and [16], where the surface tensions $\gamma_\infty^{*\prime}$ are 0.545 for $r_{\mathrm{c}}^* = 3$ and $T^* = 0.818$, and 0.55 for $r_{\mathrm{c}}^* = 2.5$ and $T^* = 0.72$.

3.2. Simulation of cylindrical vapour bubbles and the calculation of Tolman length

The selected four box sizes and numbers of particles (liquid+vapour) of simulation systems are shown in Table 1.

Table 1. Numbers of particles and the simulation domains in simulations of cylindrical vapour bubbles.

Particle numbers (N)	$L_x^* \times L_y^* \times L_z^*$
16848	$15.0 \times 40.0 \times 40.0$
19656	$15.0 \times 45.0 \times 45.0$
24204	$15.0 \times 50.0 \times 50.0$
29952	$15.0 \times 55.0 \times 55.0$

Some details of the establishment of vapour bubbles are indicated as follows.

(i) In the simulation domains introduced in Table 1, the particles are distributed uniformly. Then by running MD the system tends towards a sub-stable equilibrium liquid state with pressure smaller than the saturation pressure at $T^* = 0.75$.

(ii) A short-range repulsive force in radial direction, which is independent of z direction and direction angle, is applied near z axis, which leads to a cylindrical vapour bubble.

(iii) When the cylindrical vapour bubble is formed and the equilibrium is reached, the force field is removed, and then a new equilibrium is reached quite quickly. An example of a cylindrical vapour bubble is shown in Fig. 2.

Then we perform statistics on the physical quantities of the systems. For example the normal component of the pressure tensor of a cylindrical vapour bubble is calculated according to Eq. (17) shown below, and then the surface tension is calculated according to Eq. (9).

To calculate the normal components of the pressure tensor of the cylindrical vapour bubble, we insert 36 cylinders with the same central axis z and different radius r_k^* $(k = 1, 2, \ldots, 36)$, spaced evenly by separation Δr^* in the simulation domain except the region next to the box wall. In a way similar to that to deduce the normal components of the pressure tensor of spherical liquid in Ref. [17], it is easy to prove that the normal component of the pressure tensor for our k-th cylinder layer $p_{\mathrm{N}}^*(r_k^*)$ is

$$P_{\mathrm{N}}^*(r_k^*) = \langle n^*(r_k^*)\rangle_{[r_k^*\pm(1/2)\Delta r^*]} T^* - \frac{1}{2\pi r_k^{*2} L_z^*}\left\langle \sum_{i,j} \frac{\boldsymbol{r}_k^* \cdot \boldsymbol{r}_{ij}^*}{r_{ij}^*} U^{*\prime}(r_{ij}^*)\, g_{k,ij} \right\rangle. \quad (17)$$

The first term on the right-hand side of Eq. (17) is the kinetic term of the k-th cylinder shell $p_k(r)$. $\langle n^*(r_k^*)\rangle_{[r_k^*\pm(1/2)\Delta r^*]}$ denotes the time average of the particle number density $n^*(r_k^*)$ in the cylindrical layer with thickness being Δr^* and the middle surface being the k-th cylinder (with radius r_k^*). The second term is configurational term $p_{\mathrm{U}}^*(r)$. $U^*(r_{ij}^*)$ is the interparticle potential function. $\boldsymbol{r}_{ij}^*$ and r_{ij}^* are the relative vector and distance between two particles (i, j). $\boldsymbol{r}_k^*$ is the position vector of the intersection or one of the two position vectors of the intersections between the link of (i, j) and the k-th cylinder. $g_{k,ij}$ is the number of intersections between the link of (i, j) and the k-th cylinder. Figure 4 gives the results of the configurational term $p_{\mathrm{U}}^*(r)$, the kinetic term $p_{\mathrm{K}}^*(r)$, and their sum $p_{\mathrm{N}}^*(r)$ in radial direction of the cylindrical vapour bubble for 24024 particles at $T^* = 0.75$.

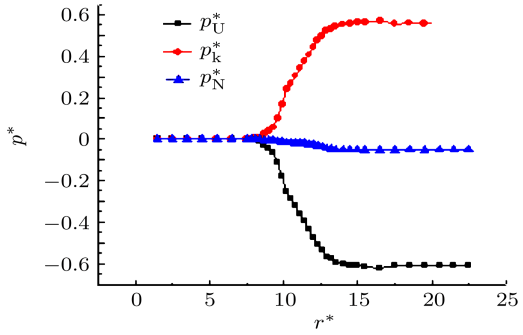

Fig. 4. (colour online) Pressure distribution of $N = 24024$ system.

Substituting the result of $p_{\mathrm{N}}^*(r_k^*)$ from Eq. (17) into Eq. (9) gives the surface tension γ_{s}^*. Then by substituting this γ_{s}^* and pressures inside vapour and liquid bulks respectively given by Eq. (17), p^{v*} and p^{l*} into Eq. (8), the radius of surface of tension R_{s}^* is obtained. Substituting the results R_{s}^* and γ_{s}^* into Eq. (4) with $\gamma_\infty^* = 0.5896$, we obtain four approximate values for the Tolman length for four different systems, respectively. Besides, we fit the values of four different bubble systems and the planar interface system into Eq. (4), and obtain a more reliable Tolman length $\bar{\delta}_\infty^* = -0.6225$. These results are shown in Table 2, from which we can see that our result of $\bar{\delta}_\infty^* = -0.6225$ is close to the result ~ -0.75 shown in Fig. 8 of Ref. [11] and obviously different from the result (nearly zero) of Ref. [1]. Besides, our result of Tolman length being negative for an Ar vapour bubble is also consistent with that of Block *et al.*'s[18] treatment by surface free energy: "present evidence that for $R \to \infty$ the leading order (Tolman) correction for droplets has sign opposite to the case of bubbles".

Table 2. Results of four cylindrical bubbles and the planar vapour–liquid interface system.

N	ρ_l^*	ρ_v^*	$(p^v)^* - (p^l)^*$	γ_s^*	R_s^*	δ_∞^*
16848	0.7355	0.0001	0.064	0.631	9.859	–0.6921
19656	0.7369	0.0001	0.059	0.629	10.661	–0.7036
24024	0.7408	0.0001	0.056	0.623	11.125	–0.6293
29952	0.7412	0.0001	0.051	0.615	12.058	–0.5185
12672	0.7556	0.0111	0	0.5896	∞	$\bar{\delta}_\infty^* = -0.6225$

4. Explanation of the origin of the Tolman length difference in the literature

In Ref. [1], the liquid pressure was evaluated with the virial expression, which was negative in general and was found to be strongly dependent on R_s. The vapour pressure was estimated from the vapour density via an empirical equation of state given by their MD simulation for the bulk vapour phase. The vapour pressure thus obtained was found to be independent of R_s and very close to the vapour pressure in bulk liquid–vapour equilibrium. Then they used the Y–L equation (7) to calculate the surface tension of the bubble γ_s, which turned out to be also independent of R_s. This means that the Tolman length is nearly zero. This contradicts the results of Ref. [11] and ours. It seems to us that this contradiction is probably attributed to the empirical equation of state used in the calculation of vapour in Ref. [1]. The empirical equation of state obtained from their MD simulation for bulk vapour can be applied only to the case where the boundary effect can be neglected, while the bubbles in Ref. [1] are so small that the effect of the vapour–liquid boundary on the internal vapour in the bubble cannot be neglected. Therefore the empirical equation of state is invalid for the bubbles discussed there. The second cause may lie in the fact that the difference between the surface tension and an equimolar surface was ignored in Ref. [1].

5. Conclusions

Since disputes continue as to whether and how the surface tension of nanobubbles varies with curvature radius, we carry out MD study on cylindrical vapour bubbles of argon instead of the spherical bubbles used in the other literature to reduce the statistical error. We report on the values of radius of surface tension R_s and surface tension γ_s of four different systems, respectively, with numbers of molecules 16848, 19656, 24024, and 29952 at temperature $T = 90$ K. Besides, we obtain the surface tension for planar surface γ_∞ by MD simulation. These data show that the surface tension decreases with radius increasing. By fitting the Tolman equation $\gamma_s/\gamma_\infty = 1/(1 + \delta_\infty/R_s)$ for a cylindrical surface with our data, the Tolman length $\bar{\delta}_\infty = -0.6225\sigma$ is given, where $\sigma = 0.3405$ nm is the diameter of argon atom. The zero Tolman length given by Ref. [1] is negated and it is pointed out that this error is attributed to the application of the inapplicable empirical equation of state and the neglect of the difference between surface of tension and equimolar surface in Ref. [1].

References

[1] Matsumoto M and Tanaka K 2008 *Fluid Dyn. Res.* **40** 546

[2] Tsai J C, Kumar M, Chen S Y and Lin J G 2007 *Sep. Purif. Technol.* **58** 61

[3] Dupont V, Miscevic M, Joly J L and Platel V 2003 *Int. J. Heat Mass Transfer* **46** 4245

[4] Yang J W, Duan J M, Fornasiero D and Ralston J 2003 *J. Phys. Chem.* B **107** 6139

[5] Tolman R C 1949 *J. Chem. Phys.* **17** 333

[6] Rowlinson J S and Widom B 1982 *Molecular Theory of Capillarity* (New York: Oxford University Press)

[7] Lu H M and Jiang Q 2005 *Langmuir* **21** 779

[8] Protasova L N, Rebrow E V, Ismagilov Z R and Schouten J C 2009 *Micropor. Mesopor. Mat.* **123** 243

[9] Prylutskyy Y I, Matzui L Y, Gavryushenko D A Sysoev V M and Scharff P 2005 *Fuller. Nanotub. Car. N.* **13** 287

[10] Zhu R Z, Cui S W, Yan H, Yang Q W and Wen Y H 2007 *Fuller Nanotub. Car. N.* **6** 417

[11] Park S H, Weng J G and Tien C L 2001 *Int. J. Heat Mass Transfer* **44** 1849

[12] Nijmeijer M J P, Bruin C, van Woerkom A B and Bakker A F 1992 *J. Chem. Phys.* **96** 565

[13] Kim B G, Lee J S, Han M H and Park S 2006 *Nanosci. Microsci. Therm.* **10** 283

[14] Allen M P and Tildesley D J 1989 *Computer Simulation of Liquids* (New York: Oxford University Press)

[15] Wei J A 2005 "Theories and Molecular Dynamics of Cylindrical Droplets and Their Contact Phenomena on Solid Surface", *Master Dissertation* (Advised by professor Zhu Ru-Zeng) Beijing, China

[16] Nijmeijer M J P, Bakker A F, Bruin C and Sikkenk J H 1988 *J. Chem. Phys.* **89** 3789

[17] Thompson S M, Gubbins K E, Walton J P R B, Chantry R A R and Rowlinson J S 1984 *J. Chem. Phys.* **81** 530

[18] Block B J, Das S K, Oettel M, Virnau P and Binder K 2010 *J. Chem. Phys.* **133** 154702